

# Mapping Hydrothermal Mineral Deposits Using PCA and BR Methods in Baft 1:100000 Geological Sheet, Iran

Amirmohammad Abhary, Hossein Hassani

Amirkabir University of Technology, Department of Mining and Metallurgical Engineering, Tehran, Iran

**Abstract**— Evaluating the conventional methods for mapping hydrothermal altered deposits by using landsat-8 OLI images in the Baft one to one hundred thousand geological Sheet is the prime target of our study. We used the color composite, band ratio, principal component analysis. The color composite and band ratio methods showed very clearly the hydrothermal altered deposits of clay minerals, iron oxides and ferric oxides around the fumaroles. The principal component analysis also enabled us to represent undoubtedly the altered hydroxyl and iron oxide mineral deposits of this region concentrating around the fumaroles. Finally, the target detection method for reference spectral analysis by using EnvI 4.8 detected the representative hydrothermal altered minerals around study area. Therefore, all the methods showed high efficiency for mapping hydrothermal altered mineral deposits.

**Keywords**— Baft, Hydrothermal Alteration; OLI, Band Ratio, PCA.

## I. INTRODUCTION

The definition of hydrothermal alteration is the reflection of response of preexisting, rock forming minerals to physical and chemical conditions different than those, under which they originally formed, especially by the action of hydrothermal fluids[1]. The hydrothermal fluid processes alter the mineralogy and chemistry of the host rocks that can produce distinctive mineral assemblages which vary according to the location, degree and duration of those alteration processes. When these alteration products are exposed at the surface, they can be mapped as a zonal pattern. They appear concentrically around a core which has the highest grade alteration and greatest economic interest. The importance of the recognition of such spatial patterns of alteration makes the 'remote sensing technique' one of the standard procedures in exploration geology, due to its high efficiency and low cost [2].

There are many studies around the world related to hydrothermal alteration mapping using multispectral satellite images especially, Landsat and Aster (e.g., [3]–

[6]). Thematic mapping multispectral images from Landsat satellites cover the visible and infrared spectrum of hydrothermal alterations [7], [8]. The major types of alteration found in volcanic areas are potassic, phyllic, argilic, propylitic, and silicification. Each type of alteration has diagnostic minerals in their respective rocks. Satellite imaging plays an efficient role in differentiating the representative minerals for the different types of alterations. Hydrothermal alteration could also be used to locate faults in any volcanic area. Usually, the alteration zones are correlated with the discharged flows from the volcanic reservoir, and with the main structures that control the permeability of the reservoir and the cap rock. So, locating hydrothermally altered rocks in the surface can help to determine the presence of up flows from the volcanic reservoir.

Previous studies explained the fact that certain minerals associated with hydrothermal processes, such as iron bearing minerals (e.g., goethite, hematite, jarosite and limonite) and hydroxyl bearing minerals (e.g., kaolinite and K-micas) show diagnostic spectral features that allow their remote identification [9]. Iron oxide is quite a common constituent of alteration zones associated with hydrothermal sulphide deposits [10]. The major iron oxide species – goethite, jarosite, and hematite that are formed from the weathering of sulfides absorb energy at different frequencies in the VNIR/SWIR [11], providing a means of discrimination using hyperspectral scanners [12]. Hydroxyl bearing minerals form the most widespread product of alteration.

The main target of our study is to detect and map the hydrothermal altered minerals in study area by using satellite imaging information by the conventional methods, i.e., color composites, band ratio, PCA.

Fig.1 shows the Location of our study area.

## II. LANDSAT-8 OLI/TIRS DATA

Landsat-8 images of Baft area was obtained from the US Geological Survey Earth Resources Observation and Science Center (<http://earthexplorer.usgs.gov>). The image

map projection is Universal Transverse Mercator zone 40N (polar stereographic for Antarctica) from the WGS 84 datum. The OLI features two additional spectral channels with advanced measurement capabilities: a deep blue band for coastal water and aerosol studies (band 1, 0.433–0.453 m, 30 m pixel size), and a band for cirrus cloud detection (band 9, 1.36–1.39 m, 30 m pixel size). The TIRS collects data in two long wavelength thermal bands (band 10, 10.30–11.30 m, 100 m pixel size; band 11, 11.50–12.50 m, 100 m pixel size), which have been co-registered with OLI data. Table 1 shows Landsat-8 OLI properties.

### III. PRE-PROCESSING OF LANDSAT-8 OLI/TIRS DATA

The Landsat-8 image of the target site was processed with Environment for Visualizing Images version 4.8 software. Landsat-8 data were converted to surface reflectance by the internal average relative reflection method [13], which is recommended for calibration in mineralogical mapping, as it does not require prior knowledge of samples collected in the field. During atmospheric correction, raw radiance data from an imaging spectrometer is rescaled to reflectance data, and therefore all spectra are shifted to nearly the same albedo. The resulting spectra can be compared directly with laboratory or field reflectance spectra. Panchromatic and cirrus cloud bands were not used in this study.

### IV. COLOR COMPOSITES

Three additive colors (i.e., red, green and blue) were used to display multispectral bands in the color composite method where the spectral response of the minerals indicates a maximum in their reflectance. This enhancement is achieved by combining bands in the visible and the infrared portion [14].

### V. BAND RATIO

The band ratio is a technique that has been used for many years in remote sensing to display spectral variations effectively (e.g., [15]). It is based on highlighting the spectral differences that are unique to the materials being mapped. Identical surface materials can give different brightness values because of the topographic slope and aspect, shadows, or seasonal changes in sunlight illumination angle and intensity.

These variances affect the viewer's interpretations and may lead to misguided results. Therefore, the band ratio operation could be able to transform the data without reducing the effects of such environmental condition.

In addition, ratio operation may also provide unique information that is not available in any single band which is very useful for disintegrating the surface materials [16].

The band ratio images are known for enhancement of spectral contrasts among the bands considered in the ratio operation and have successfully been used in mapping of alteration zones [17].

### VI. PRINCIPAL COMPONENT ANALYSIS (PCA)

The principal components analysis (PCA) uses the principal components transformation technique for reducing dimensionality of correlated multispectral data. The analysis is based on multivariate statistical technique that selects uncorrelated linear combinations (eigenvector loadings) of variables in such a way that each successively extracted linear combination, or principal component (PC), has a smaller variance [18]. The statistical variance in multispectral images is related to the spectral response of various surficial materials such as rocks, soils, and vegetation, and it is also influenced by the statistical dimensionality of the image data [19]. Eigenvector loadings (eigenvalues) give information using magnitude and sign of about which spectral properties of vegetation, rocks and soils are responsible for the statistical variance mapped into each PC, and this is the basis of the Crosta technique.

### VII. DISCUSSION

In the case of Color composites Fig. 2 shows hydrothermal alteration zone as deep green and blue (RGB as 5:7:3).

From the theoretical knowledge of mineral's spectral properties, it is well recognized that the Landsat-8 bands

ratios of  $(\frac{4}{2}, \frac{6}{7}, \frac{6}{5})$  are analyzed for iron oxides, hydroxyl bearing minerals, ferrous oxides, respectively.

The applied Abrams ratio  $(\frac{6}{7}, \frac{4}{3}, \frac{5}{6})$  illustrated the

hydrothermal altered iron oxide as green and clay minerals as red color (Fig. 3). Minerals containing iron ions, vegetated zones and hydroxyl minerals show respectively red, green and blue color using Kaufmann

ratio  $(\frac{7}{5}, \frac{5}{4}, \frac{6}{7})$  (Fig. 4). Using Chica-Olma ratio  $(\frac{6}{7}, \frac{6}{5}, \frac{4}{2})$ , altered clay minerals as will be obtained red, iron

ions as green and ferrous oxide as blue color (Fig. 5). From these entire analysis maps, the region with high concentrated iron minerals was found.

In the case of Principal component analysis (PCA), it could be predicted that iron oxides will be distinguished by bright pixels in PC4 of Table 2

(Fig.6). Hydroxyl bearing minerals are mapped as dark pixels in PC5 due to the fact that the contribution is negative from Band 6 and positive from Band 7 in this PC, so they could be shown by bright pixels in -PC5 Form (Fig.7).

Note that in this project, band 6 has been used as background for a better illustration of minerals, so the bright pixels will be shown by rainbow colors.

### VIII. CONCLUSIONS

We evaluated the applicability of Landsat-8 data for obtaining geological information on hydrothermal alteration, with selected image-processing methods. In the study area, Landsat-8 bands yielded information that allowed identification of vegetation, iron oxide and hydroxide and clay and carbonate minerals, silicate mineral and lithological units for the exploration of Hydrothermal deposits.

After using the conventional alteration mapping methods on the Landsat image in the study area, we found that the color composite and band ratio methods showed their efficiency to define the area of hydrothermal alteration. Principal component analysis illustrated the iron oxides and hydroxyl altered minerals area of this region very clearly. We have mapped successfully the spatial distribution of goethite, hematite and clay minerals of our study area using conventional methods. In conclusion, we found all of the hydrothermally altered minerals in study area. So, it is quite clear that all these methods are quite efficient to delineate hydrothermal alteration products using Landsat-8 OLI images in study area.

### REFERENCES

- [1] R. E. Beane, "Hydrothermal alteration in silicate rocks, southwestern North America; In:," *Advances in Geology of the Porphyry Copper Deposits, Southwestern North America*: Tucson (ed.) Titley S R, Univ. Ariz. Press, Chapter 6, pp. 117–137, 1982.
- [2] E. Yetkin, "Alteration Mapping By Remote Sensing: Application To Hasandağ–Melendiz Volcanic Complex, M.Sc. Thesis, Middle East Technical University, Ankara, Turkey, 97p." 2003.
- [3] M. G. Abdelsalam, R. J. Stern, and W. G. Berhane, "Mapping gossans in arid regions with Landsat TM and SIR-C images: the Beddaho Alteration Zone in northern Eritrea," *J. African Earth Sci.*, vol. 30, no. 4, pp. 903–916, 2000.
- [4] T. M. Ramadan, M. G. Abdelsalam, and R. J. Stern, "Mapping gold-bearing massive sulfide deposits in the Neoproterozoic Allaqi Suture, Southeast Egypt with Landsat TM and SIR-C/X SAR images," *Photogramm. Eng. Remote Sensing*, vol. 67, no. 4, pp. 491–497, 2001.
- [5] A. Madani, E. M. Abdel Rahman, K. M. FA WZY, and A. Emam, "Mapping of the hydrothermal alteration zones at Haimur gold mine area, South Eastern Desert, Egypt, using remote sensing techniques," *Egypt. J. Remote Sens. Sp. Sci.*, vol. 6, pp. 47–60, 2003.
- [6] T. M. Ramadan and A. Kontny, "Mineralogical and structural characterization of alteration zones detected by orbital remote sensing at Shalatein District, SE Desert, Egypt," *J. African Earth Sci.*, vol. 40, pp. 89–99, 2004.
- [7] G. R. Hunt and R. P. Ashley, "Spectra of altered rocks in the visible and near infrared," *Econ. Geol.*, vol. 74, pp. 1613–1629, 1979.
- [8] G. R. Hunt, "Near-infrared (1.3-2.4)  $\mu\text{m}$  spectra of alteration minerals-Potential for use in remote sensing," *Geophysics*, vol. 44, no. 12, pp. 1974–1986, 1979.
- [9] G. R. Hunt, "Electromagnetic radiation: The communication link in remote sensing," *Remote Sens. Geol. Siegal B S Gillespie A R (New York Wiley)*, 1980.
- [10] P. R. and O. M. M, "Detection minerals by advanced spectral analysis in ETM+ imagery," *Proceeding 7th Iran. Student Conf. Min. Eng. Tabriz*, pp. 111–119, 2009.
- [11] L. C. Rowan, "Near infrared iron absorption bands: Applications to geologic mapping and mineral exploration;," *Remote Sens. Watson Regan; Society Explor. Geophys. Repr. Ser.*, vol. 3, pp. 250–268, 1983.
- [12] D. L. Taranik, F. A. Kruse, A. F. H. Goetz, and W. W. Atkinson, "Remote sensing of ferric iron minerals as guides for gold exploration; Proceedings Eighth Thematic Conference on Geologic Remote Sensing, Denver, Colorado," pp. 197–228, 1991.
- [13] E. Ben-Dor, F. A. Kruse, A. B. Lefkoff, and A. Banin, "Comparison of three calibration techniques for utilization of GER 63-channel aircraft scanner data of Makhtesh Ramon, Negev, Israel," *Photogramm. Eng. Remote Sensing*, vol. 60, no. 1994, pp. 1339–1354, 1994.
- [14] A. Crosta and J. Moore, "McM., Enhancement of Landsat Thematic Mapper imagery for residual soil mapping in SW Minas Gerais State, Brazil: a prospecting case history in Greenstone belt terrain," in *Proceedings of the 7th ERIM Thematic Conference: Remote sensing for exploration geology*, 1989, pp. 1173–1187.
- [15] A. F. H. Goetz, B. N. Rock, and L. C. Rowan,



“Remote sensing for exploration; an overview,”  
*Econ. Geol.*, vol. 78, no. 4, pp. 573–590, 1983.

- [16] J. R. Jensen, “Thematic information extraction: Image classification,” *Introd. Digit. Image Process. A Remote Sens. Perspect. 2nd edn*, Prentice Hall Ser. Geogr. Inf. Sci. 318p, 1996.
- [17] D. B. Segal, “Use of Landsat multispectral scanner data for the definition of limonitic exposures in heavily vegetated areas,” *Econ. Geol.*, vol. 78, pp. 711–722, 1983.
- [18] A. Singh and A. Harrison, “Standardized principal components,” *Int. J. Remote Sens.*, vol. 6, no. 6, pp. 883–896, 1985.
- [19] W. P. Loughlin, “Principal component analysis for alteration mapping,” *Photogramm. Eng. Remote Sensing*, vol. 57, no. 9, pp. 1163–1169, 1991.
- [20] “GSI (Geological Survey of Iran),” *1100,000 Baft Geol. Sheet*, 1970.

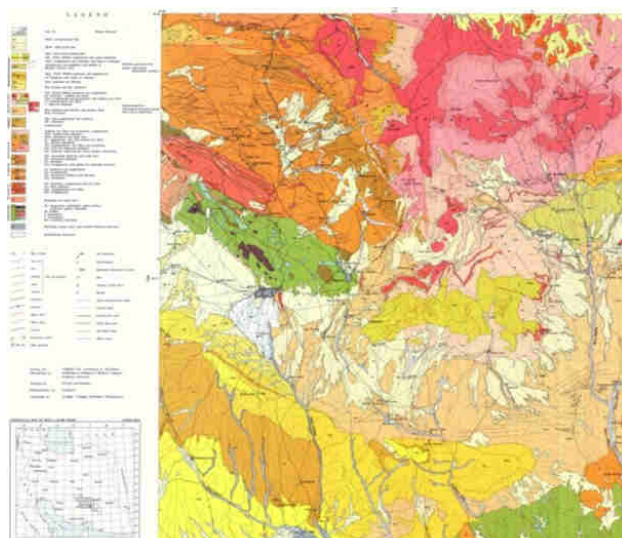


Fig.1: Location of our study area, Baft 1:100000 geological Sheet, Iran [20].

Table.1: Landsat-8 OLI properties  
(<http://landsat.usgs.gov>)

Landsat-8 OLI and TIRS Bands (μm)		
30 m Coastal/Aerosol	0.435 - 0.451	Band 1
30 m Blue	0.452 - 0.512	Band 2
30 m Green	0.533 - 0.590	Band 3
30 m Red	0.636 - 0.673	Band 4
30 m NIR	0.851 - 0.879	Band 5
30 m SWIR-1	1.566 - 1.651	Band 6
100 m TIR-1	10.60 – 11.19	Band 10
100 m TIR-2	11.50 – 12.51	Band 11
30 m SWIR-2	2.107 - 2.294	Band 7
15 m Pan	0.503 - 0.676	Band 8
30 m Cirrus	1.363 - 1.384	Band 9

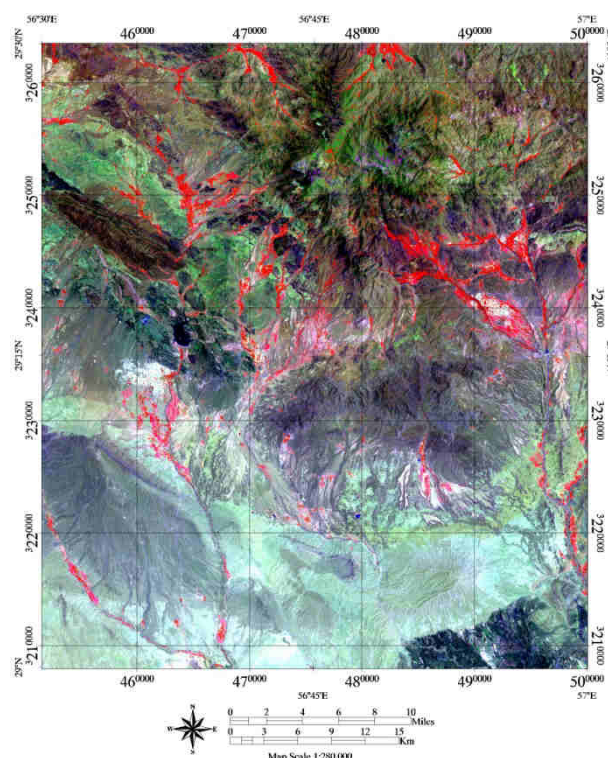


Fig.2: Hydrothermal alteration zone as deep green and blue (RGB as 5:7:3)

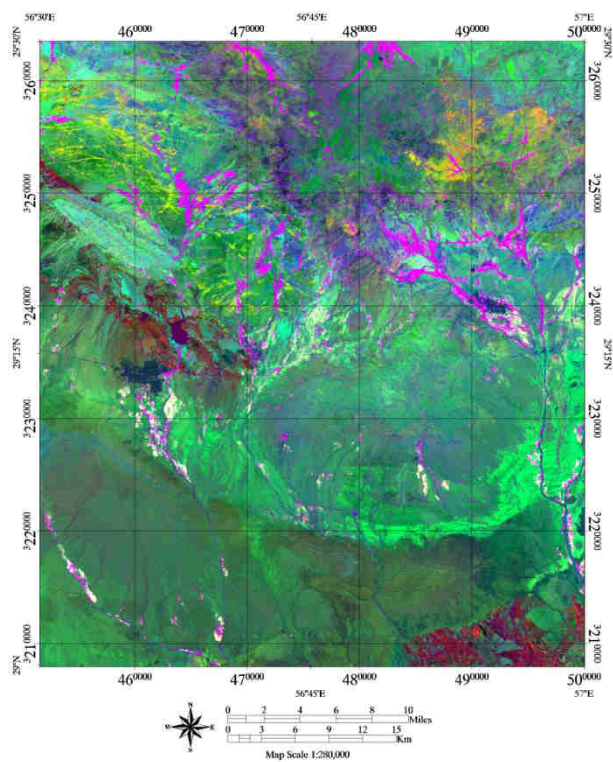


Fig.3: Abrams ratio ( $\frac{6}{7}, \frac{4}{3}, \frac{5}{6}$ ) illustrated the hydrothermal altered iron oxide as green and clay minerals as red color

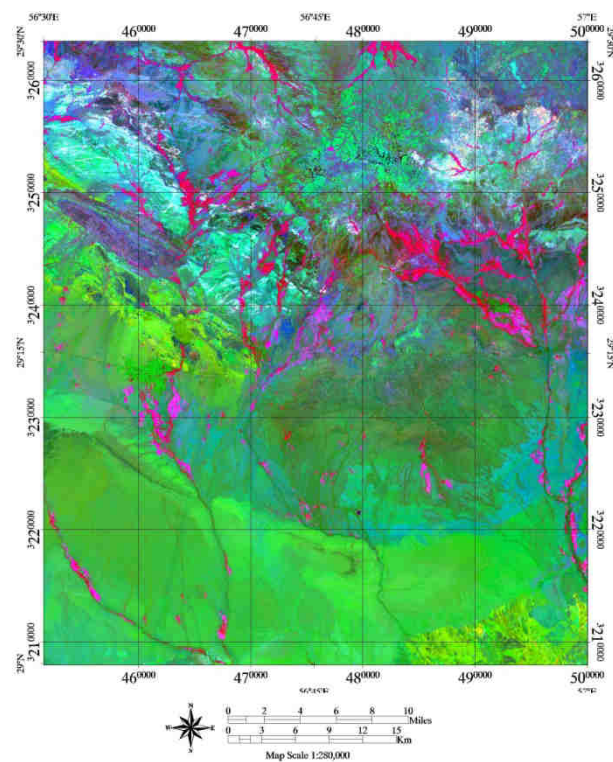


Fig.5: Altered clay minerals as red, iron ions as green and ferrous oxide as blue color Chica-Olma ratio ( $\frac{6}{7}, \frac{6}{5}, \frac{4}{2}$ )

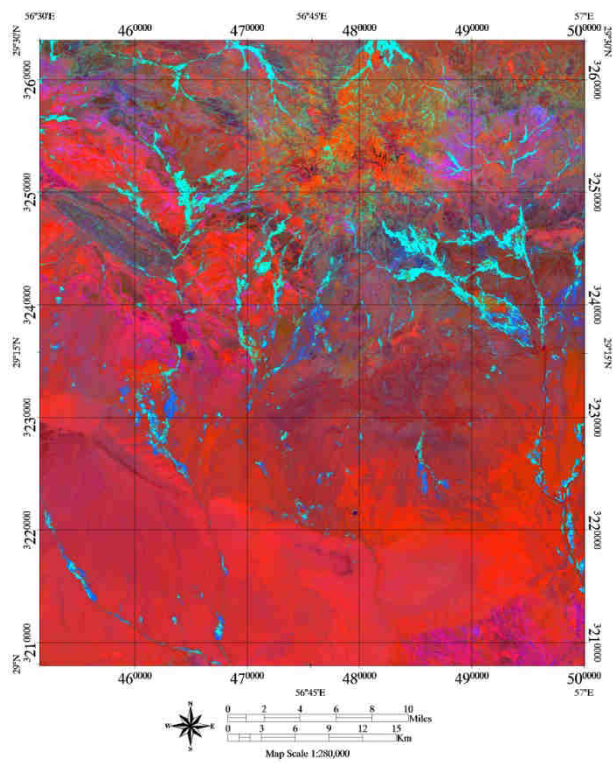


Fig.4: Minerals containing iron ions, vegetated zones and hydroxyl minerals show respectively red, green and blue color using Kaufmann ratio ( $\frac{7}{5}, \frac{5}{4}, \frac{6}{7}$ )

Table.2: PCA analyses results for study area

Band 7	-0.528746	-0.210509	-0.471170	-0.373699
Band 6	-0.506132	0.095810	-0.474562	0.277981
Band 5	-0.331408	0.885275	0.256754	-0.137316
Band 4	-0.413866	-0.221254	0.392849	0.688471
Band 3	-0.338261	-0.200807	0.374596	-0.135537
Band 2	-0.262147	-0.271141	0.438424	-0.521400
Eigenvector r	PC 1	PC 2	PC 3	PC 4



	0.558856	0.046285
	-0.647656	-0.112739
	0.146083	-0.018395
	0.333306	-0.200861
	-0.236263	0.794194
	-0.282787	-0.560107
PC 5		
PC 6		

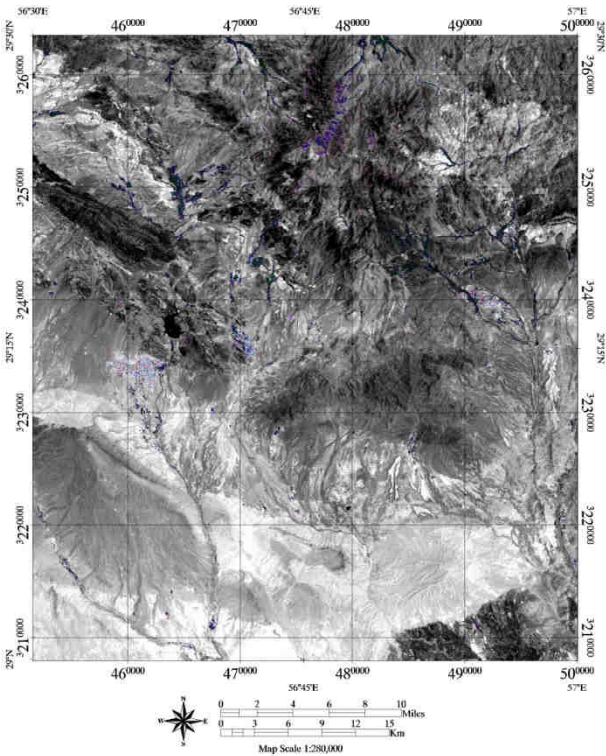


Fig.6: Iron oxides are distinguished by rainbow colors in PC4

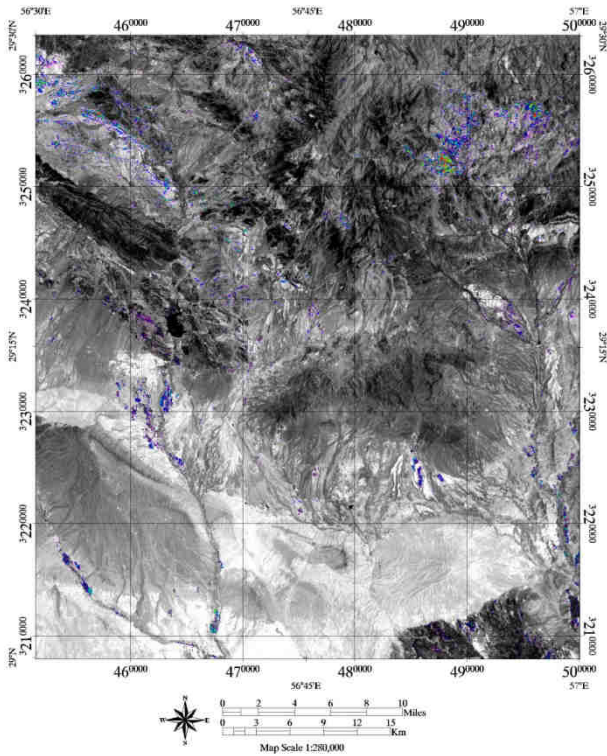


Fig.7: Hydroxyl bearing minerals by rainbow colors in –PC5